AGU PUBLICATIONS

JGR

Journal of Geophysical Research: Oceans

RESEARCH ARTICLE

10.1002/2016JC012043

Key Points:
- Fallout from thermonuclear testing entrained bomb-produced carbon-14 to the sea surface
- A Guam coral stored carbon-14 signals from operation-specific thermonuclear testing
- Ocean current modeling provided validation of hypothesized fallout carbon-14 transport

Supporting Information:
- Supporting Information S1

Correspondence to:
A. H. Andrews,
Allen.Andrews@noaa.gov

Citation:
Andrews, A. H., R. Asami, Y. Iryu, D. R. Kobayashi, and F. Camacho (2016), Bomb-produced radiocarbon in the western tropical Pacific Ocean: Guam coral reveals operation-specific signals from the Pacific Proving Grounds, *J. Geophys. Res. Oceans*, *121*, 6351–6366, doi:10.1002/2016JC012043.

Received 7 JUN 2016
Accepted 1 AUG 2016
Accepted article online 6 AUG 2016
Published online 27 AUG 2016

Bomb-produced radiocarbon in the western tropical Pacific Ocean: Guam coral reveals operation-specific signals from the Pacific Proving Grounds

Allen H. Andrews[1], Ryuji Asami[2], Yasufumi Iryu[3], Donald R. Kobayashi[1], and Frank Camacho[4]

[1]NOAA Fisheries-Pacific Islands Fisheries Science Center, Honolulu, Hawaii, USA, [2]Department of Physics and Earth Sciences, Faculty of Science, University of the Ryukyus, Nishihara, Japan, [3]Institute of Geology and Paleontology, Graduate School of Science, Tohoku University, Sendai, Japan, [4]Biology Program, College of Natural and Applied Sciences, University of Guam, Guam, USA

Abstract High-resolution radiocarbon (^{14}C) analyses on a coral core extracted from Guam, a western tropical Pacific island, revealed a series of early bomb-produced ^{14}C spikes. The typical marine bomb ^{14}C signal—phase lagged and attenuated relative to atmospheric records—is present in the coral and is consistent with other regional coral records. However, ^{14}C levels well above what can be attributed to air-sea diffusion alone punctuate this pattern. This anomaly was observed in other Indo-Pacific coral records, but the Guam record is unmatched in magnitude and temporal resolution. The Guam coral $\Delta^{14}C$ record provided three spikes in 1954–1955, 1956–1957, and 1958–1959 that are superimposed on a normal ^{14}C record. Relative to mean prebomb levels, the first peak rises an incredible ~700‰ and remained elevated for ~1.2 years. A follow up assay with finer resolution increased the peak by ~300‰. Subsequent spikes were less intense with a rise of ~35 and ~70‰. Each can be linked to thermonuclear testing in the Pacific Proving Grounds at Bikini and Enewetak atolls in Operations Castle (1954), Redwing (1956), and Hardtack I (1958). These ^{14}C signals can be explained by vaporization of coral reef material in the nuclear fireball, coupled with neutron activation of atmospheric nitrogen (^{14}C production), and subsequent absorption of $^{14}CO_2$ to form particulate carbonates of close-in fallout. The lag time in reaching Guam and other coral records abroad was tied to ocean surface currents and modeling provided validation of ^{14}C arrival observations.

1. Introduction

Hermatypic corals have provided numerous records for bomb-produced radiocarbon (^{14}C) in tropical seas of the world and can function as archives in marine science. Typically reported as $\Delta^{14}C$ in reference to a prenuclear standard [*Stuiver and Polach*, 1977], these records can provide proxies for mixed layer ventilation processes and as a reference for environmental ^{14}C levels over time [*Broecker and Peng*, 1982; *Druffel*, 1997]. The tropical marine bomb ^{14}C signal is typically attenuated and phase lagged relative to the atmospheric record and each region has its own amplitude and temporal characteristics [*Druffel*, 2002; *Grottoli and Eakin*, 2007]. This observation emphasizes the challenges for use of this kind of record as a reference in determining the age of fishes [*Kalish*, 1993; *Andrews et al.*, 2011] and other tropical marine organisms [*Fallon and Guilderson*, 2005; *Darrenougue et al.*, 2013; *Van Houtan et al.*, 2016] that form conserved hard parts (i.e., otoliths or skeletal structures). Because of its efficacy in providing validated age and growth estimates for marine organisms that require management, bomb ^{14}C dating using hermatypic corals as a reference has expanded in its application geographically and in its temporal utility [e.g., *Cook et al.*, 2009; *Andrews et al.*, 2012, 2013, 2015; *Vitale et al.*, 2016]. The aim of the current study was to establish a new $\Delta^{14}C$ record for Guam—a benchmark for future age and growth studies in the region—using an existing coral core from Guam that was previously analyzed and validated ($\delta^{18}O$) as a temporal record for ocean-climate change [*Asami et al.*, 2004, 2005], historical plutonium (Pu) sources [*Lindahl et al.*, 2011], and ocean acidification [*Shinjo et al.*, 2013].

Based on general latitudinal trends in seawater $\Delta^{14}C$ of the Pacific Ocean—attributed to CO_2 saturation states of tropical versus temperate waters [*Broecker and Peng*, 1982]—it was hypothesized that the bomb ^{14}C pattern for Guam would lie between existing coral $\Delta^{14}C$ records from locations north and south of Guam. The coral records from Okinawa [*Konishi et al.*, 1982] and Hawaii (French Frigate Shoals (FFS) and Kure Atoll) [*Druffel*, 1987;

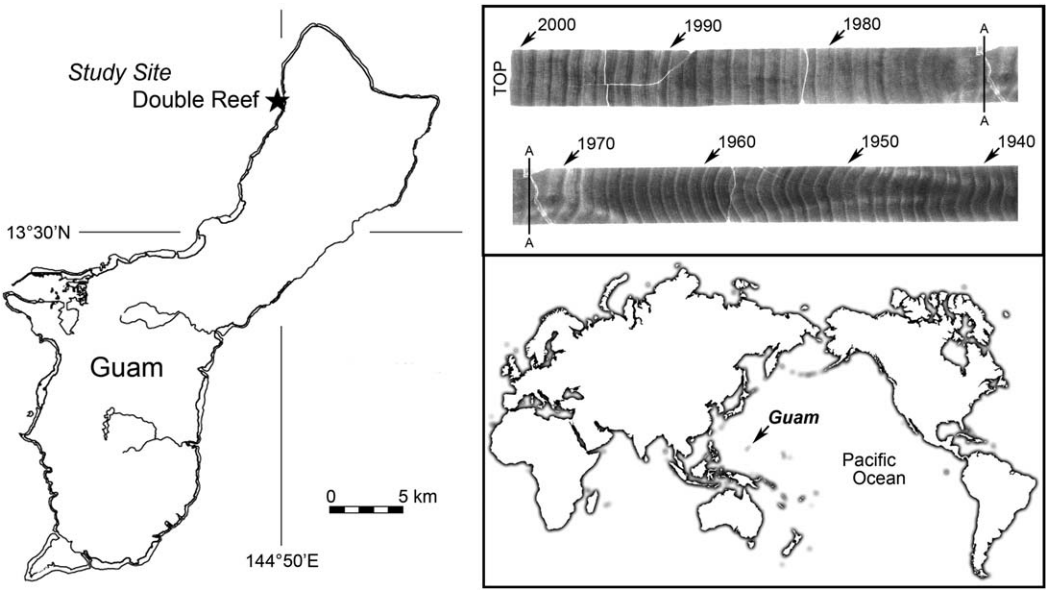

Figure 1. Location of Guam with regional map showing study site where the coral core was extracted. Inset of the coral core X-ray was limited to the sample period (1939–2000). Double reef is offshore and well exposed to oceanic waters.

Andrews et al., 2016] were expected to be the greatest and timeliest due to their more northerly position (between 25°N and 30°N). The Δ^{14}C coral record for Nauru (0.5°S) exemplifies a southern hemisphere signal [*Guilderson et al.*, 1998]—defined as more deeply phase lagged and attenuated—by residing near the equator and separated oceanographically from North Pacific waters by the North Equatorial Current (NEC) and North Equatorial Counter Current (NECC). A recent coral Δ^{14}C record from Palau [*Glynn et al.*, 2013] was expected to be most similar to Guam in timing and amplitude due to its down-current position within the NEC (~1200 km southwest of Guam). In addition, it was hypothesized that an early bomb ^{14}C signal, similar to what was observed at Palau and attributed to close-in fallout [*Glynn et al.*, 2013], would be detected in the Guam coral core because of its close proximity to Bikini and Enewetak atolls (~2000 km due east of Guam)—the most westerly location of the US Pacific Proving Grounds (PPG) where several military operations were conducted in the 1950s to test thermonuclear devices [*Hansen*, 1988]. Herein we generate a high-resolution (ca. monthly to bimonthly) Δ^{14}C time series in a coral core from Guam. Given an early bomb ^{14}C signal was observed, the goals of this study were to describe the source dynamics—its temporal characteristics relative to known nuclear testing dates and current patterns across the western Pacific and into the Indo-Pacific region—by utilizing other more distant coral records that have also registered an early bomb ^{14}C signal [i.e., *Konishi et al.*, 1982; *Fallon and Guilderson*, 2008; *Guilderson et al.*, 2009; *Druffel-Rodriguez et al.*, 2012; *Glynn et al.*, 2013].

2. Materials and Methods

2.1. Coral Core

The coral skeleton core selected to establish the Δ^{14}C time series was originally collected from Double Reef on the northwestern shore of Guam in the western tropical Central Pacific on 5 April 2000 (Figure 1). The core was 273 cm in length and was extracted from a hemispherical coral colony (*Porites lobata*) that was 3.3 m high with a bottom depth of 7.8 m. The annual periodicity of the growth band pattern was previously analyzed using δ^{18}O as a proxy for temperature and salinity and could be used as a validated basis for the Δ^{14}C time series [*Asami et al.*, 2004, 2005]. The timespan of the entire core (years 1787–2000) greatly exceeded what was necessary to establish a bomb ^{14}C time series. Hence, the most recent ~60 years (1939–2000) was chosen to adequately cover the prebomb period through to the peak period, and then into the post-peak decline.

2.2. Coral Microsampling

Sample extraction across the coral core slab was performed manually with the aid of a Minimo drill (Model C101) on a vertical press-mount (Minitor Co., Ltd., Japan) in a HEPA filtered clean bench. Samples were in

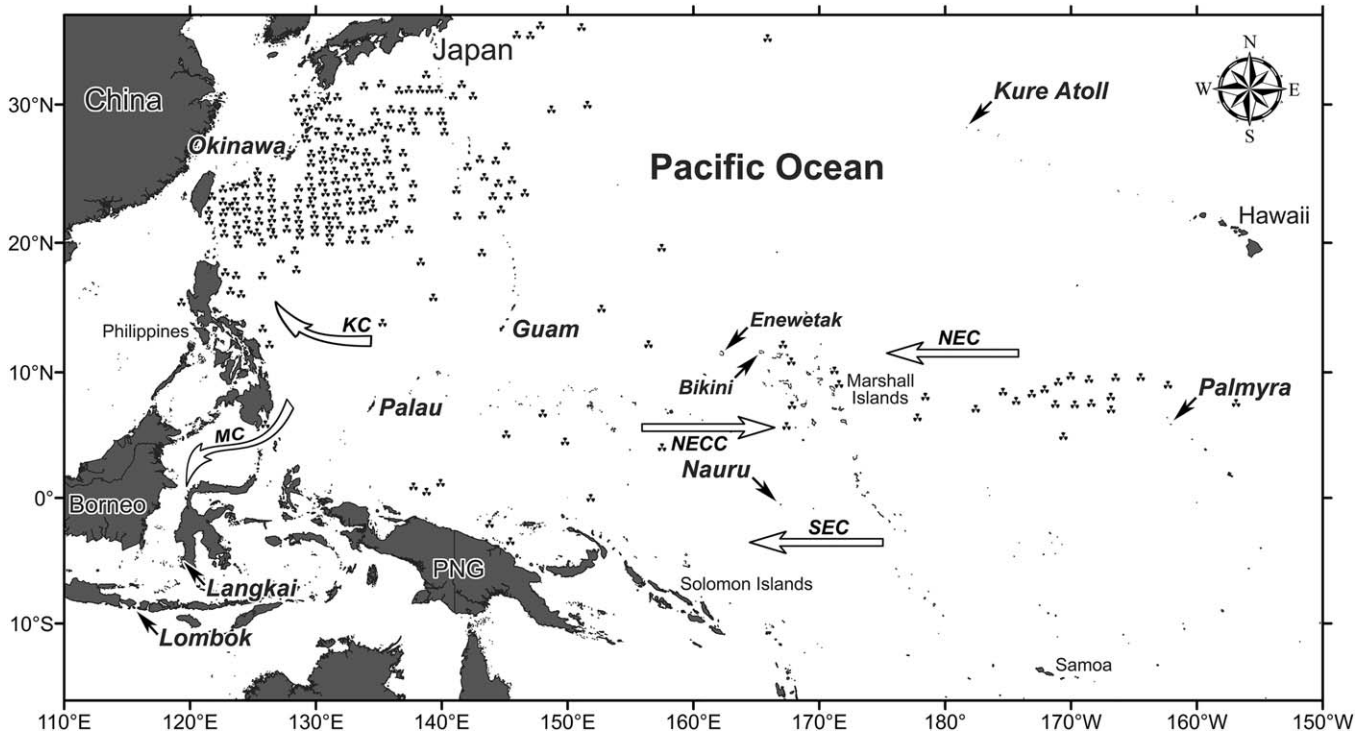

Figure 2. Map of the central western Pacific Ocean and Indo-Pacific covering the locations of coral ^{14}C records of interest to this study with generalized surface currents. The Kure Atoll ^{14}C record provided a well-mixed ^{14}C record indicative of northern hemisphere air-sea diffusion. Other coral ^{14}C records confirmed transport of a fallout signal to Palau via NEC, Okinawa via Kuroshio Current (KC), Langkai Island and Lombok Strait via Mindanao Current (MC), and Palmyra via North Equatorial Countercurrent (NECC). South Equatorial Current (SEC) provides an effective barrier to N-S transport (not present in Nauru coral). The strongest radioactive signal was traced in March–June 1954 by Japanese researchers (nuclear symbols = radioactive fish, boats, or water)—surface transport was apparent to the northwest, southwest, and southeast [*Nishiwaki*, 1955; *Sevitt*, 1955].

the form of powder extracted from small adjacent holes in series, ranging from the youngest to oldest part of the coral core during the period of interest. Sampling was performed with a 2.7 mm diamond end mill (Minitor Co., Ltd., Japan) for the years 2000–1971, after which a 2 mm end mill was employed for the remainder of the time series for greater temporal resolution (1970–1939). Samples extracted in this manner were transferred as powder to polypropylene vials (1.5 mL snap-cap centrifuge tubes) with a target weight of ~4 mg per sample (specific sample weights were not measured). After each extraction, the end mill was cleaned in dilute HCl, rinsed in Milli-Q water (18.2 MΩ), and dried with filtered, oil-less compressed air. The coral slab was also cleaned for residual sample extraction powder with filtered, oil-less compressed air prior to the next extraction.

Upon discovery of $\Delta^{14}C$ levels that greatly exceeded expectations in the 1950s, the decision was made to resample this portion of the coral core at a higher temporal resolution. This series of samples was extracted with a 0.9 mm end mill in the same manner as described previously, but at 2× the number of original samples for each of the three $\Delta^{14}C$ spike regions.

The extracted powder samples were submitted as carbonate to the National Ocean Sciences Accelerator Mass Spectrometry Facility (NOSAMS), Woods Hole Oceanographic Institution (WHOI), Woods Hole, MA, for routine radiocarbon analysis using Accelerator Mass Spectrometry (AMS). Radiocarbon measurements were reported by NOSAMS as Fraction Modern ($F^{14}C$) after correction for fractionation using measured $\delta^{13}C$ [*Reimer et al*., 2004]. These $F^{14}C$ values were used to calculate age-corrected $\Delta^{14}C$ [*Stuiver and Polach*, 1977] using validated date of coral formation for direct comparison with other $\Delta^{14}C$ records.

2.3. Other Regional $\Delta^{14}C$ Records

To provide a regional context to the Guam $\Delta^{14}C$ reference, other coral records from previous studies were considered (Figure 2). The closest complete records were from Okinawa and Hawaii (FFS and Kure Atoll) to the north and Nauru and Palau to the south [*Konishi et al*., 1982; *Druffel*, 1987; *Guilderson et al*., 1998; *Glynn et al*., 2013; *Andrews et al*., 2016]. Two fragment records were also available from Pohnpei (1971–1979)

Table 1. Data From Surface Thermonuclear Tests That Exceeded a Yield of 1 Mt at PPG in the 1950s[a]

Operation	Shot	Date	Yield	Height	Type	Location
Ivy	Mike	31/10/52	10.4		Surface	Enewetak
Castle	Bravo	28/2/54	15	7 (2)	Surface	Bikini
	Romeo	26/3/54	11	14 (4)	Barge	Bikini
	Union	25/4/54	6.9	13 (4)	Barge	Bikini
	Yankee	4/5/54	13.5	14 (4)	Barge	Bikini
	Nectar	13/5/54	1.69	14 (4)	Barge	Enewetak[b]
Redwing	Zuni	27/5/56	3.5	9 (3)	AD-surface	Bikini
	Dakota	25/6/56	1.1		Barge	Bikini
	Apache	8/7/56	1.85		Barge	Enewetak
	Navajo	10/7/56	4.5		Barge	Bikini
	Tewa	20/7/56	5.0		Barge	Bikini
Hardtack I	Fir	11/5/58	1.36	10 (3)	Barge	Bikini
	Koa	12/5/58	1.37	3 (1)	Surface	Enewetak
	Oak	28/6/58	8.9	8.6 (3)	Barge	Enewetak
	Poplar	12/7/58	9.3	12 (4)	Barge	Bikini
	Pine	26/7/58	2.0	8 (3)	Barge	Enewetak

[a]These tests were most significant in providing regional close-in fallout. All other nuclear tests were <500 kt and were mostly within the largest test timespans (Table S1). Date is GCT (Greenwich Civil Time) and Yield is megatons (TNT equivalent). Height in feet (meters) and AD = airdrop.

[b]Often reported as Bikini, but confirmed as Enewetak from aerial survey flight data [*LeVine and Graveson*, 1954].

[*Konishi et al*., 1982] and the southwestern coast of Guam at Taelayag Reef (1978–1981) [*Moore et al*., 1997], each of which provided some initial information on how the full bomb ^{14}C curve may behave for Guam. All records were used to contrast the amplitude and timing of the Guam $\Delta^{14}C$ rise and peak.

The discovery of three $\Delta^{14}C$ spikes in the 1950s led to an in-depth examination of nuclear testing at Bikini and Enewetak atolls and a comparison to updated atmospheric records [*Hua et al*., 2013]. Unclassified information on nuclear tests was examined for indications of when the spikes were created and how they may be tied to operation-specific testing in the region [*Department of Energy*, 1994; *Yang et al*., 2000]. Because interaction of the nuclear fireball with a land or sea surface is necessary for high levels of close-in fallout, the focus was on operation shots that were near and exceeding 1 Mt—most of which were at or near the surface of land, lagoon, or sea (Table 1)—to establish the greatest potential contributions to each $\Delta^{14}C$ spike. In addition, documentation of fallout processes was examined for information that may explain the direct infusion of ^{14}C to the marine environments of Bikini and Enewetak atolls. Finally, other $\Delta^{14}C$ coral records from farther abroad were considered in describing the movement of the first and strongest $\Delta^{14}C$ signal (Operation Castle) through stratified ocean surface currents to other locations in the central Pacific and Indo-Pacific regions. Depth profiles and current modeling were used to validate the transport mechanism and timing.

2.4. Ocean Current Transport Modeling

To provide an estimate of fallout particle propagation, Lagrangian transport simulations were conducted using ocean currents from a comprehensive ocean reanalysis called the Simple Ocean Data Assimilation version 2 (SODA2) [*Carton et al*., 2000]. SODA2 was chosen for this study because it is a comprehensive reconstruction of the ocean state in the past century (SODA2 v.2.2.4; NetCDF format from Asia-Pacific Data-Research Center, International Pacific Research Center, University of Hawaii at Manoa; http://apdrc.soest.hawaii.edu/). This model output covers the period 1871–2010 at monthly 0.5° latitude/longitude resolution, and 39 layers of vertical resolution. The thickness of the top 10 layers (upper 121 m) ranges from 10.0 m at the surface to 16.3 m at depth. These strata were as assumed to represent the mixed layer of the ocean surface and would cover the lower limit of density gradients observed after fallout events [*Nishiwaki*, 1954; *Miyake and Saruhashi*, 1958]. The modeling was a simplified approach that used an isobaric transport model (i.e., particles remained at a particular depth strata); however, it was safe to assume that the depth strata were initial starting points that became well mixed over the transport distances and could reach near surface depths for accretion into the shallow water corals, which is plausible due to typical mixed layer dynamics over great distances.

The transport modeling was accomplished using Lagrangian individual-based movement dynamics at a 1 day time step with a diffusivity parameter of 250 $m^2 \cdot s^{-1}$. This value of diffusivity was chosen based upon

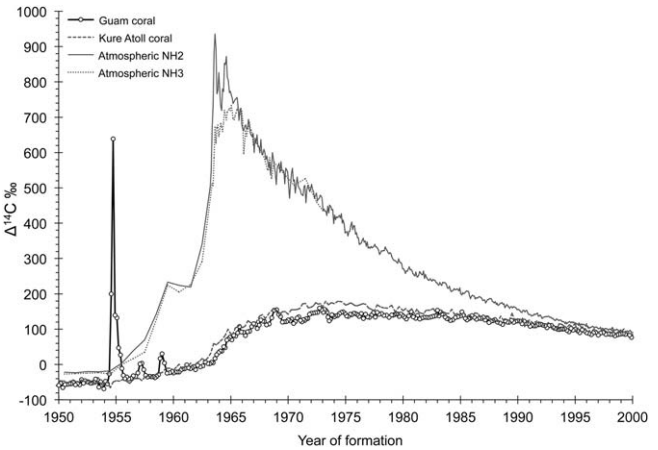

Figure 3. Plot of the new $\Delta^{14}C$ record from Guam with two atmospheric records and the Kure Atoll $\Delta^{14}C$ record [*Andrews et al.*, 2016]. The unexpectedly high spike from the Guam coral, followed by two smaller spikes, was more than can be explained by air-sea diffusion alone. The Kure Atoll record exemplifies the expected marine ^{14}C signal (no spikes). The largest spike approached maximum atmospheric $\Delta^{14}C$ levels at ~640‰ and can be linked to close-in fallout from nuclear testing at the US Pacific Proving Grounds in the Marshall Islands. Atmospheric records were plotted to cover the region of interest (~140°E–170°E) [*Hua et al.*, 2013].

analysis of NOAA drifter buoys [*Rivera et al.*, 2011]. This simulation was written in Python with data visualizations accomplished with mapping software Generic Mapping Tools [*Wessel and Smith*, 1991]. Particles were released for each blast event (Table 1), using a 200 nautical mile (322 km) radius circle as a particle seeding point, and centered on each blast location. Circle size was chosen based on unknown effects of differential atmospheric dispersal prior to transport mediated by ocean currents; however, evidence from fallout studies from various blast events provided evidence that the most significant fallout would have been closest to ground zero. A large number of replicates were desirable to adequately characterize the variability of particle transport given there is a random, diffusive component to movement dynamics (i.e., particles released at same point in time and space may not follow similar paths). The sample size used (n = 5000 per event) was chosen based on previous experience with transport modeling and constraints imposed by computational logistics [e.g., *Wren and Kobayashi*, 2016]. Particle proximities to any of the coral core locations were tabulated daily if the particle was within 100 km. Particles were at liberty for 3 years, but this was a modeling constraint and not an actual lifespan (duration was long enough to characterize primary transport pathways). The time series of particle hits was scaled to the yield (Mt) of the particular blast event. In this manner, the time series of relative particle hits could be directly compared to the coral ^{14}C time series at each same location. This comparison, coupled with the initial depth strata scenarios (10 layers at 0–121 m), allowed inference of the likely transport pathways used by the blast event particles. Analysis of modeling results focused on arrival time and the initial depth strata that correlated with observed coral core ^{14}C data. Modeled arrival for Guam focused on all three operations, while the other locations may or may not have included other operations.

3. Results

3.1. Guam Coral ^{14}C Record

Extracted samples from the Guam coral core numbered 370, with one sample (GD2-346) lost during processing, for a total of 369 ^{14}C measurements covering the years 1939–2000 (National Centers for Environmental Information, NESDIS, NOAA, U.S. Department of Commerce; https://www.ncdc.noaa.gov/paleo/study/20346). The number of samples per year of coral growth varied from 4.5 to 9.5 based on the annual bandwidth for the given period and the end mill diameter. The $\Delta^{14}C$ values determined from these measurements ranged from a prebomb low of −78.4‰ in 1940 to a maximum value of 638.9‰ in 1954—well beyond what was expected for an early ^{14}C spike. Three spikes were observed in 1954–1955, 1956–1957, and 1958–1959 as superimposed peaks on the pre-bomb to initial $\Delta^{14}C$ rise levels from air-sea diffusion of $^{14}CO_2$ (Figure 3). Relative to mean prebomb levels measured in the Guam coral core (−60.8 ± 4.9‰; n = 84 and pre-1952), the first peak rises abruptly by ~710‰ and remained elevated for ~1.2 years before returning to initial bomb ^{14}C rise levels. Subsequent spikes were less intense with a rise of ~35 and ~70‰ above expected levels (Figure 3). The continuity of the Kure Atoll $\Delta^{14}C$ record [*Andrews et al.*, 2016] was used as a reference for a gradual $\Delta^{14}C$ rise from air-sea diffusion (Figures 3 and 4). As hypothesized, the gradual $\Delta^{14}C$ rise and peak for Guam was between the northern (Okinawa and Hawaii) and southern (Nauru) records, and most similar to Palau (Figure 4). Short records from Pohnpei [*Konishi et al.*, 1982] and Guam

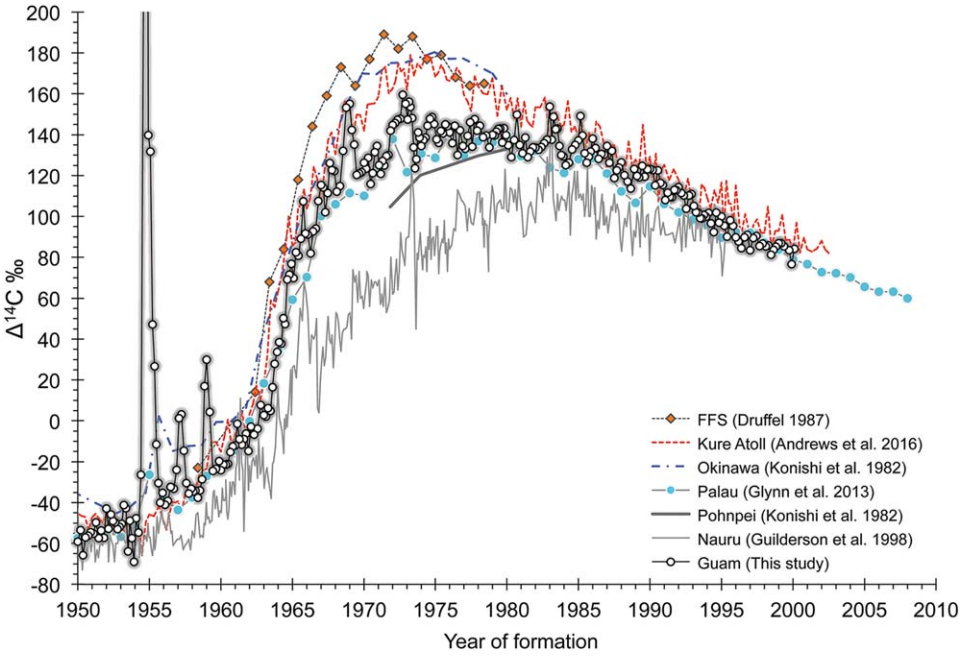

Figure 4. Plot of the new Guam $\Delta^{14}C$ record (shadowed open circles) with other regional coral $\Delta^{14}C$ records that surround Guam. As predicted by its intermediate latitudinal position, the Guam record was between the timeliest records from the northern Pacific and the attenuated and phase-lagged records south of the equatorial Pacific. Palau was most similar in timing and amplitude. The short Pohnpei record shows the effect of moving closer to Guam from the south. A short record from Guam (1978–1981) [*Moore et al*., 1997] was not plotted to reduce complexity, but was consistent with the new record. The early spike is truncated to focus on the overall ^{14}C patterns of each record.

[*Moore et al*., 1997] were also consistent with the new Guam record. The Pohnpei $\Delta^{14}C$ rise was lagged a few years later but rises to meet the Guam record, which would be expected for its position farther south. The new Guam $\Delta^{14}C$ record was similar on average to the short Guam record (1978–1981; $138.2 \pm 6.0‰$ cf. $136.4 \pm 11.5‰$, respectively; not plotted in Figure 4 due to visual complexity).

In general and ignoring the ^{14}C spikes, the Guam coral $\Delta^{14}C$ record rises slowly to a maximum as a 16 year plateau with a mean $\Delta^{14}C$ of 137.5‰ and punctuated with a series of widely separated spikes to ~150‰ in the early 1970s and 1980s (Figure 4). As expected, the broad peak for Guam is different from the more accentuated peaks of Okinawa and Hawaii. Kure Atoll provided the most comprehensive data set for a North Pacific coral record and contrasts from the Guam record by having a narrow peak near 175‰ for a period of less than 2 years [*Andrews et al*., 2016]. Mean prebomb for Guam was $-54.3 \pm 4.9‰$ from 1939 to 1952, the year of the first thermonuclear test (Operation Ivy, Mike Shot). This value is lower than prebomb calculated for the same period at Kure Atoll ($-46.6 \pm 4.9‰$) and Okinawa ($-41.5 \pm 3.6‰$), and most similar to prebomb for Palau ($-54.7 \pm 2.1‰$). The total $\Delta^{14}C$ increase between the means of Guam prebomb and peak was ~200‰ in ~17 years (1952–1969), compared to ~220‰ in ~20 years (1952–1973) for Kure Atoll. The period and rate for the most rapid $\Delta^{14}C$ increase were similar: Guam = 44.8‰ per year (1962.75–1964.75) and Kure Atoll = 45.0‰ per year (1963.46–1965.75). Relative to the lower resolution records of Okinawa and Hawaii (FFS), the rise rates were also similar but precede the Guam rise period by 1–2 years. Palau rises earlier but tapers off later than Guam (Figure 4). After the broad 16 year plateau for Guam, $\Delta^{14}C$ tapers off slowly and irregularly into the postpeak decline period (after ~1986–1990). At this point in time, the Guam $\Delta^{14}C$ record runs in parallel with the Kure Atoll and Palau records.

3.2. Guam Coral ^{14}C Record and Nuclear Testing

Each of the three $\Delta^{14}C$ spikes measured in the Guam coral can be linked directly to testing of thermonuclear devices in the PPG at Bikini and Enewetak atolls (Tables 1 and S1 and Figure 5). The largest $\Delta^{14}C$ spike—an increase of ~700‰ above prebomb levels—can be linked to Operation Castle (28 March to 13 May 1954), where a series of six nuclear tests released a total yield of ~48.09 Mt, of which three tests exceeded 10 Mt (Shots Bravo, Romeo, and Yankee). The second $\Delta^{14}C$ spike is lowest of the three—an increase of

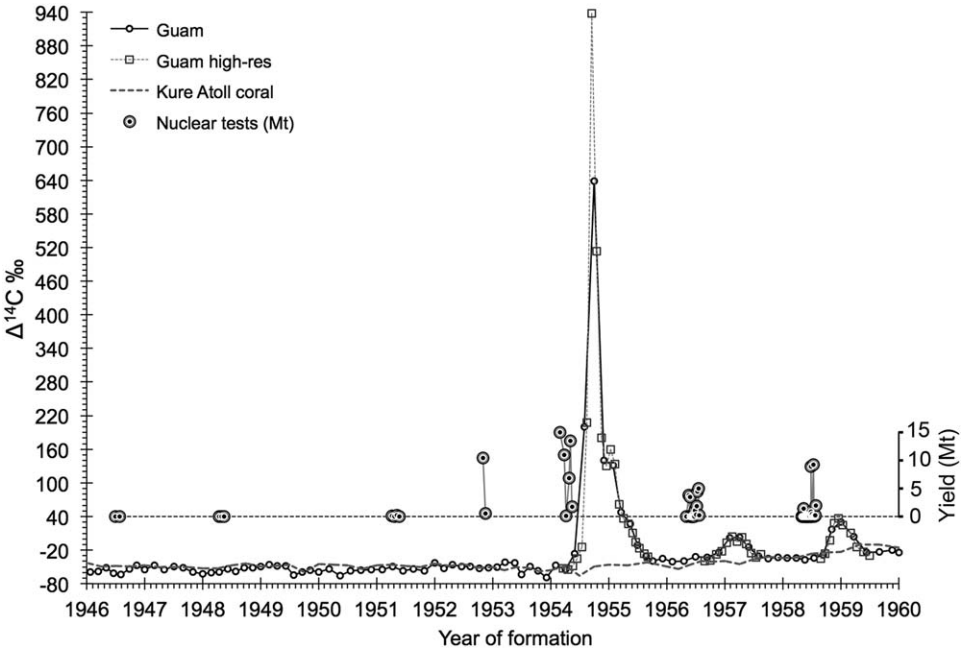

Figure 5. Plot of the new $\Delta^{14}C$ record from the Guam coral focusing on the three spikes measured in the 1950s. The high-resolution sample series confirmed the observations and included a spike increase in 1954–55 ($\sim$940‰). The Kure Atoll record exemplifies the levels expected from air-sea diffusion. In concert with the Guam coral $\Delta^{14}C$ spikes, a second scale is plotted in correlated time to show the nuclear test operations at the PPG. Each symbol represents the yield of individual tests in the megaton (Mt) range (right vertical scale bar). Early nuclear tests during Operations Crossroads (1946), Sandstone (1948), and Greenhouse (1951) were not of significant magnitude to produce a $\Delta^{14}C$ signal in seawater reaching Guam (Table S1). Operation Ivy (1952) produced the first thermonuclear explosion, but did not register in the Guam coral. Nuclear tests conducted for Operations Castle (1954), Redwing (1956), and Hardtack I (1958) were of much greater cumulative magnitude (Table 1), each of which produced a measureable $\Delta^{14}C$ spike.

$\sim$35‰ above air-sea diffusion levels—and can be linked to Operation Redwing (4 May to 21 July 1956), where a series of 17 nuclear tests released a total yield of $\sim$20.8 Mt. All tests in Operation Redwing were $\leq$5 Mt. The final spike was during the initial $\Delta^{14}C$ rise period and exceeded the trend by $\sim$70‰, which can be attributed to Operation Hardtack I (28 April to 26 July 1958). This series consisted of 31 successful nuclear tests for a total yield of $\sim$26.6 Mt, of which two tests were just under 10 Mt (Shots Oak and Poplar). Operation Hardtack I was the last of the nuclear test operations at Bikini and Enewetak atolls (future PPG tests were high altitude off Johnston Atoll and open ocean shots under Operation Dominic).

Resampling of the three $\Delta^{14}C$ spikes at higher temporal resolution (2×; n = 42) led to verification of the measurements made for 1956–1957 and 1958–1959, and provided an large increase to the observed peak levels in 1954–1955 (Figure 4; https://www.ncdc.noaa.gov/paleo/study/20346). Peak values for the 1956–1957 spike were similar in magnitude with a peak period dip to -4.8‰ ($\sim$February–May 1957). A sharper peak was recorded for the 1958–1959 spike ($\Delta^{14}C = 36.4$‰ cf. 30.0‰). The peak value for the 1954–1955 spike exceeded the initial measurements by $\sim$300‰ ($\Delta^{14}C = 638.9$‰ cf. 937.6‰) in mid-September 1954. Conformity of the higher resolution samples with the initial measurements was good, but the initial rise was earlier (1954.4 cf. 1954.5)—this difference is likely negligible because of the limits to temporal resolution in the coral records.

3.3. Bomb-Produced ^{14}C and Ocean Currents

The movement of seawater masses containing the operation-specific ^{14}C signals to Guam and other locations were measured based on observed arrival dates of the ^{14}C spikes in coral core records (Figure 2). Guam was the only location where each nuclear test operation was resolved. This observation is consistent with a direct entrainment of a fallout ^{14}C signal in the NEC from Bikini and Enewetak to Guam (Figure 6), followed by a dispersal of the ^{14}C signals to the northwest (Kuroshio Current), southwest (Minandao Current) and southeast (NECC; Figure 2). In addition, regional sampling performed in 1954 and 1955 by Japanese researchers provided the locations of radioactive fish, fishing boats, or water samples—a timely distribution of the bomb-produced plume (a mix of radioisotopes (e.g., ^{65}Zn, ^{90}Sr) that would include ^{14}C)

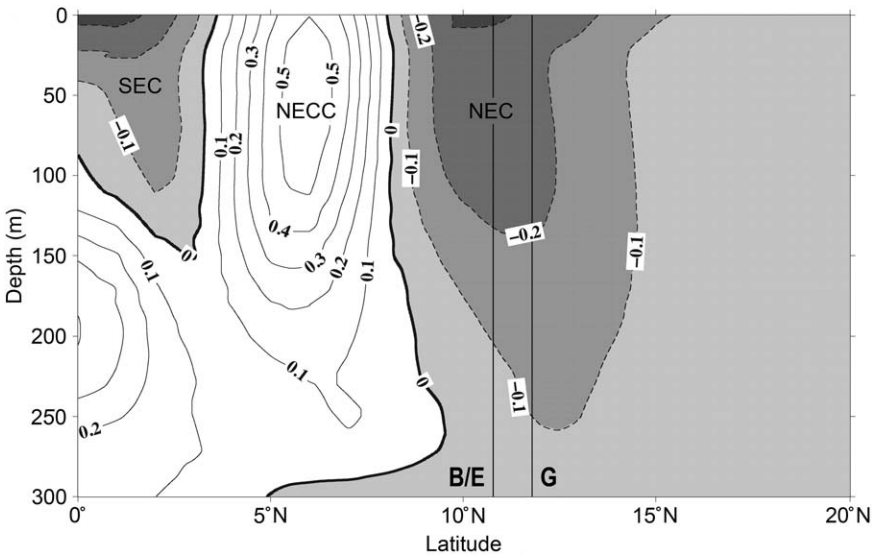

Figure 6. Profile of east-west current patterns (grey scale = westward direction) to a depth of 300 m for region between PPG and Guam (140°E–170°E). The latitude of Bikini and Enewetak (B/E) and Guam (G) demonstrate that the North Equatorial Current (NEC) provided a direct avenue for transport of nuclear fallout to Guam. SEC = South Equatorial Current (SEC) and NECC = North Equatorial Countercurrent (NECC). Current speeds are in $m \cdot s^{-1}$ along the respective contours.

created by close-in fallout from Operation Castle (Figure 2) [*Nishiwaki*, 1955; *Sevitt*, 1955; *Miyake and Saruhashi*, 1958].

By tracing the arrival times of each operation-specific ^{14}C signal in the Guam coral core, estimates of the time and speed required to transport the signal were derived and rounded off to the most significant figure because of uncertainties in the time of coral formation for each measurement (Table 1 and Figure 7).

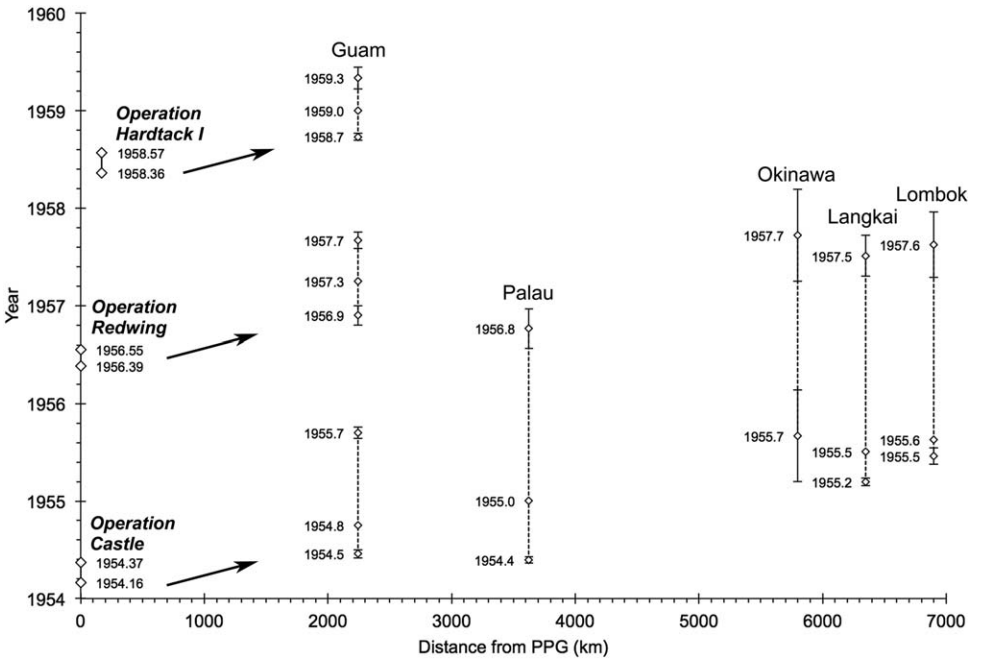

Figure 7. Propagation over distance and time of the operation-specific ^{14}C signals—elevated levels preserved in coral—to Guam and more distant locations. Shown on left are original timespans for nuclear test operations with corresponding spikes observed in Guam. Spike periods observed in coral are plotted left to right at each location relative to distance from the PPG. Transport of ^{14}C from Operations Redwing and Hardtack I were not observed beyond Guam. Timespans represent initial arrival, highest peak value (midpoint, if present), and a return to air-sea diffusion levels.

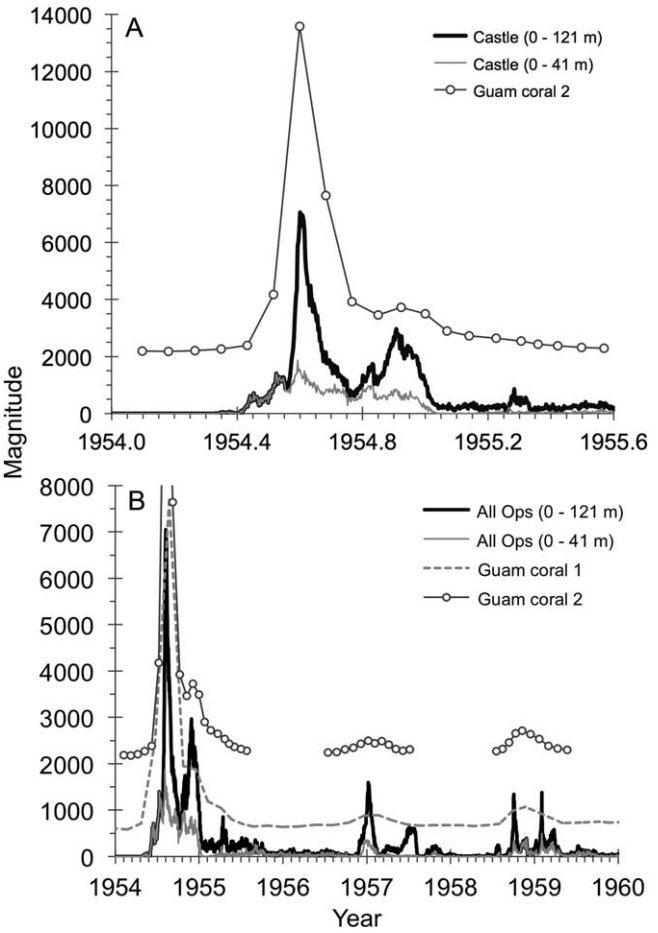

Figure 8. Modeling of bomb-produced ^{14}C arrival at (A) Guam from Operation Castle and (B) Operations Redwing and Hardtack I with the two Guam coral core ^{14}C records (Guam coral 1 = first samples; Guam coral 2 = high resolution). Initial depth strata for each operation are plotted together (0–121 m), with surface depths separated (0–41 m) to highlight the timing and relative contribution. A minor time adjustment of −0.1 years was made to the Guam coral records for peak alignment. Magnitude is modeling counts and an arbitrarily transformed value for coral ^{14}C records to emphasize temporal alignment.

Distance traveled for Operations Castle and Redwing was 2240 km (Bikini to Guam) and was an average of distances from Bikini and Enewetak (2070 km) for Operation Hardtack I due to a mix of test sites. The ^{14}C signal from Operation Castle (76 day test period) arrived at Guam in approximately ~3 months for a mean current speed of ~0.2–0.3 m·s^{-1} and a spike duration of ~1.3 years. Operations Redwing (61 day test period) and Hardtack I (76 day test period) took more time to arrive at approximately 5–6 months and 4–5 months, respectively. As a result, mean current speeds were lower (~0.1–0.2 m·s^{-1}) with peak durations of ~0.8 and ~0.6 years, respectively.

By focusing on the largest $\Delta^{14}C$ signal in 1954–1955, a timeline was established to Guam and onward to other locations where coral $\Delta^{14}C$ records also exhibit the early ^{14}C signal (Figure 7). Palau is located in the boundary of the NEC and the NECC—downstream from Guam—and is the first to exhibit the Operation Castle ^{14}C signal after Guam [*Glynn et al.*, 2013]. The arrival of the ^{14}C spike was ~3 months after the beginning of Operation Castle and similar to the arrival for Guam, with a duration of ~2.4 years (Figure 7). Calculated mean current speed was ~0.4 m·s^{-1} (~3400 km from Bikini), which is a reasonable estimate considering the uncertainties in arrival timing from coral samples. The next record of a ^{14}C spike is with two complicated, low-resolution records from Okinawa [*Konishi et al.*, 1982]. The records were variable and somewhat contradictory, but each provided evidence of an arrival near 1955.7 ± 0.5 years (1 year sample extraction). As a result, the earliest arrival may have been ~1955.2 (transit ~380 day), but the mean arrival near 1955.7 (transit ~560 days) led to a more reasonable current speed of ~0.1–0.2 m·s^{-1} (~5800 km via Guam and Kuroshio). The timing was slightly later than some of the proximate observations made by a Japanese researcher in mid to late 1954 (Figure 2) [*Nishiwaki*, 1955], but many of these observations were well offshore and there is consistency with other observations made in 1955 [*Miyake and Saruhashi*, 1958]. No additional records were available farther northwest and two western records from the South China Sea show no evidence of the 1954–1955 spike [*Southon et al.*, 2002; *Mitsuguchi et al.*, 2007], which leads to movement beyond Palau and into the Indonesian Throughflow (ITF).

Bomb ^{14}C records from coral cores at both Langkai Island (southeastern edge of Makassar Strait) and Lombok Strait (most direct opening of ITF to Indian Ocean) revealed $\Delta^{14}C$ spikes that were attributed to Operation Castle (Figure 5) [*Fallon and Guilderson*, 2008; *Guilderson et al.*, 2009]. Each spike began nearly 1 year after the first test of Operation Castle (Shot Bravo; Table 1), leading to a transit speed of ~0.2 m·s^{-1} (~6500–7000 km from Bikini via Celebes Sea and Makassar Strait). The duration of the Operation Castle signal was complicated for each location by seasonal currents, mixed water masses, and depleted ^{14}C sources,

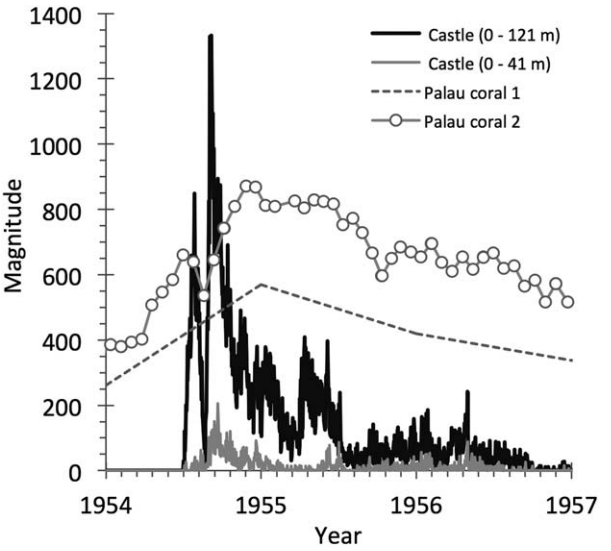

Figure 9. Modeling of bomb-produced ^{14}C arrival at Palau from Operation Castle with existing coral core ^{14}C record [*Glynn et al.*, 2013]. Initial depth strata are plotted together (0–121 m), with surface depths separated (0–41 m) to highlight the timing and relative contribution. A minor time adjustment of −0.1 years was made to align a hiatus in the Palau record with a similar observation in the modeling (notch at 1954.6). Magnitude is modeling counts and an arbitrarily transformed value for coral ^{14}C records to emphasize temporal alignment (Palau coral 1 = initial samples; Palau coral 2 = high resolution).

which could explain the punctuated spike decline [*Fallon and Guilderson*, 2008]. However, it is estimated that ^{14}C in each record begins to return to air-sea diffusion levels after ~2 years (Figure 7).

In terms of ocean transport via surface currents, the coral bomb ^{14}C record that may be the most complicated was from Palmyra Atoll. While the $\Delta^{14}C$ record from Palmyra is low resolution, a rise of up to 40‰ was attributed to nuclear testing in the PPG [*Druffel-Rodriguez et al.*, 2012]. The record appears to indicate the ^{14}C signal arrived within the first elevated sample (1955). Hence, assuming the arrival was within 6 months of the 1 year sample, transport time would be ~0.3–0.8 years. The estimate of distance traveled was not practical because of the unknowns associated where the Operation Castle plume may cross from the NEC to the NECC. In support of a close crossover to eastward movement and a rapid arrival at Palmyra, anecdotal evidence from a Japanese researcher provided measurements of radioactivity in the NECC (between Marshall Islands and Palmyra) in the months immediately after nuclear testing (Figure 2) [*Nishiwaki*, 1955].

3.4. Ocean Current Modeling and Coral ^{14}C Records

Ocean current modeling of fallout propagation from each thermonuclear test period (Operations Castle, Redwing, and Hardtack I) provided a series of transport timelines for each of the regional coral ^{14}C records with an early ^{14}C signal (Movie S1). Each simulation led to arrival times and signal magnitudes for each of 10 initial depth strata, which were then analyzed for the primary and composite depths that may have led to each coral ^{14}C signal. Of primary interest for this study were the three $\Delta^{14}C$ spikes within the Guam coral record. The arrival and strength of the modeled Operation Castle signal at Guam were well correlated with the coral ^{14}C spike and required only a minor adjustment of −0.1 year (within sample extraction error) to align the peaks (Figure 8a). Hence, the correlated arrival of the ^{14}C signal was ~1954.4. The earliest ^{14}C was from initial depths of 0–41 m, but more than 60% of the overall Castle signal was from the deepest strata (41–121 m). Results for Operations Redwing and Hardtack I were similar to the coral record, but coarser across the event timespan (Figure 8b).

The arrival of bomb-produced ^{14}C at Palau via the NEC was primarily from intermediate initial depths (41–76 m), with 91% of the overall signal from the deepest strata (41–121 m; Figure 9). Unlike the modeling results for Guam, the surface layers arrived later and contributed only 9% of the overall signal. This finding points to the importance of deep density gradients that may have been advected in subsurface currents. In addition, the modeling supports what appears to be a long spike duration of ~2.4 years. This can be attributed to the pooling effect of waters in this region (Western Pacific Warm Pool) and is exemplified by modeled particles revisiting Palau over time (Movie S1).

Modeling the transit of bomb-produced ^{14}C through the ITF provided complicated arrival details for the Langkai Island and Lombok Strait, but generally validated predictions that the previously observed spikes were from Operation Castle [*Fallon and Guilderson*, 2008; *Guilderson et al.*, 2009]. Because the coral ^{14}C records were high resolution and may have exhibited bomb-produced ^{14}C signals from all operations, the results from fallout modeling of the Redwing and Hardtack I tests were also considered (Figures 10a and 10b). Arrival of the modeled Castle signal preceded the coral records in each location by 0.5–0.7 year.

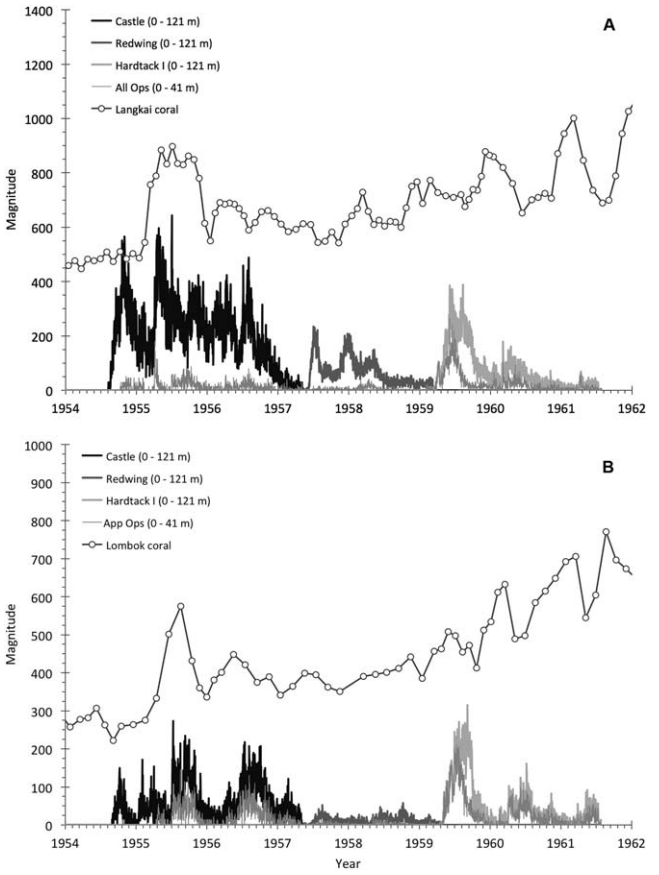

Figure 10. Modeling of bomb-produced ^{14}C arrival at (A) Langkai and (B) Lombok from Operations Castle, Redwing and Hardtack I with each respective coral core ^{14}C record [*Fallon and Guilderson*, 2008; *Guilderson et al*., 2009]. Initial depth strata for each operation are plotted together (0–121 m), with surface depths separated (0–41 m) to highlight the timing and relative contribution. Magnitude is modeling counts and an arbitrarily transformed value for coral ^{14}C records to emphasize temporal alignment.

Separation of initial surface layers (0–41 m) revealed a stronger correlation for the Lombok coral ^{14}C record with 31% of the overall signal (Figure 10a), but this scenario did not hold for the Langkai coral ^{14}C record with only 6% of the overall signal from the upper surface layers (Figure 10b). In general, the modeled signal strength was stronger for Langkai than for Lombok, which agrees with the observed $\Delta^{14}C$ increase in 1955 for both coral records ($\Delta^{14}C$ increase of $\sim$40 versus $\sim$30‰, respectively). Current modeling provided a potential explanation by showing a loss of signal strength after Langkai Island due to a split of ocean currents into the Java and Banda Seas, after being constrained by Makassar Strait (Movie S1). In general, the signals from Redwing and Hardtack I provided variable levels of input to the system and were further complicated by seasonal oscillations (Figures 10a and 10b). The ^{14}C signal from Hardtack I provided a relatively high input to the system at Langkai and Lombok with 35 and 59% of the respective signals, but Redwing was far less significant at Lombok.

The coral ^{14}C records at Okinawa and Palmyra provided the lowest temporal resolution for comparison with the modeling. There was some agreement and general confirmation of speculation that the origin of these moderate, early ^{14}C spikes was from the PPG [*Konishi et al*., 1982; *Druffel-Rodriguez et al*., 2012]. For Okinawa, the first elevated $\Delta^{14}C$ values were from Operation Castle arriving at 1955.2, which was primarily from initial sources that entered the upper surface strata (77% from 0 to 41 m). Contributions from Operations Redwing and Hardtack I were also mostly from upper surface strata and may be responsible for what appears to be a long elevated period ($\Delta^{14}C$ rise resumes $\sim$1961). This is consistent with the location of Okinawa on the western edge of the North Pacific Gyre where pooling effects were demonstrated in the particle modeling—a sustained presence of upper surface waters from the PPG (Movie S1). For Palmyra, the modeled spike could have arrived earlier by up to 1 year relative to what was recorded in the coral, but the complexity of crisscrossing waters from the NEC to the NECC likely precludes realistic arrival times (Figure 6 and Movie S1).

4. Discussion

The three spikes in marine ^{14}C that were observed in this study can be tied directly to close-in fallout from thermonuclear testing in the PPG at Bikini and Enewetak atolls of the Marshall Islands (Figure 5). The post WWII series of nuclear tests in this region mark a progression in theoretical design and maximum yield of these explosive devices over a period of 12 years [*Hansen*, 1988]. Testing in this location began with Operation Crossroads in 1946, followed by Operations Sandstone (1948) and Greenhouse (1951), all of which were fission devices of much lower yield ($\leq$225 kt) than the thermonuclear devices to follow [*Department of*

Energy, 1994] (Table S1). The first successful thermonuclear test was with the groundbreaking Mike Shot of Operation Ivy in 1952 at Enewetak Atoll with a yield of 10.4 Mt [*Gladeck et al*., 1952]. This event led a series of thermonuclear tests in this location that produced radioactive clouds that stabilized in the stratosphere (typically associated with a yield >1 Mt). As a result of these tests and others throughout the world, a global ^{14}C signal was created via stratospheric and tropospheric circulation of bomb-produced ^{14}C with uptake by land plants and soils and an eventual diffusion into the sea surface [e.g., *Nydal*, 1968; *Nydal and Gislefoss*, 1996].

The natural source of ^{14}C to the Earth-surface and marine environments is maintained by cosmic ray production of neutrons in the upper atmosphere and *n*,*p* reaction with ^{14}N to produce ^{14}C [*Libby*, 1946, 1955; *Anderson et al*., 1947]. This process results in a gradual uptake of $^{14}CO_2$ by the marine environment via air-sea diffusion [*Broecker and Peng*, 1982]. The uptake rate is exemplified in the northern tropical Pacific by the bomb-produced ^{14}C signal documented in a coral core from Kure Atoll [*Andrews et al*., 2016]. Located near the center of the North Pacific Gyre, the coral ^{14}C record shows a gradual and attenuated increase—relative to the atmospheric record—over a period of approximately 16 years before a peak is reached with a subsequent decline (Figures 3 and 4). Hence, the close concordance of the Kure Atoll record with the uninterrupted $\Delta^{14}C$ rise recorded by the Guam coral is a clear indication that air-sea diffusion alone cannot account for the three superimposed ^{14}C spikes—fallout of residual nuclear radiation with subsequent sea surface current advection to Guam must be the conduit of these anomalous signals. In addition, despite the magnitude of Mike Shot in 1952, there was no apparent bomb ^{14}C signal in the Guam coral record (Figure 5), which is an indication that a series of tests was required to create the measureable signals observed in this study.

Radioactive fallout from thermonuclear testing at Bikini and Enewetak was studied extensively by the US military and members or contractors of the Atomic Energy Commission. Almost all of the largest thermonuclear tests in this location were surface (tower or air-drop) or barge (lagoon) shots, which provided direct contact of the nuclear fireball with seawater and atoll substrates (carbonate rock, rubble, sands, and sediments of coral reefs), leading to massive close-in fallout. Cherokee Shot during Operation Redwing was a notable exception (3.9 Mt airburst at 4350 feet (1326 m)) and exemplifies the necessity of fireball surface contact by generating no significant fallout activity [*Hawthorne*, 1979]. Much of the fallout research for surface bursts was focused on how radioisotopes—created as residual radiation in a fireball that makes contact with the ground [*Glasstone*, 1964]—are propagated into the environment as an exposure hazard to humans (e.g., bone-seeking ^{90}Sr) [*Libby*, 1957, 1958; *Hawthorne*, 1979]. As a result, some of the research can be used as a proxy for how bomb-produced ^{14}C entered the sea surface directly and ended up as the signals detected at great distances in the marine environment.

Thermonuclear explosions produce an enormous burst of neutrons within the first few microseconds, most of which are immediately absorbed by atmospheric nitrogen, creating a ^{14}C source in the atmosphere immediately surrounding the fireball [*Latter and Plesset*, 1960; *Glasstone*, 1964]. While much of the ^{14}C production in these thermonuclear explosions is entrained into the superheated, toroidal cloud and advected well into the stratosphere [*Latter and Plesset*, 1960], a substantial amount will return to the surface of the Earth as close-in fallout [*Libby*, 1958; *Broecker and Walton*, 1959]. Most important in this regard is the entrainment of pulverized and vaporized surface materials (i.e., coral reef carbonates) into the superheated cloud that would provide a mix of surfaces and condensates with which the newly created $^{14}CO_2$ can react and become an integrated part of particulate fallout. In particular, it has been proposed that high heat decomposition of coral carbonates ($CaCO_3$) would produce calcium oxide (CaO), some of which is subsequently rehydrated to calcium hydroxide ($Ca(OH)_2$), which would combine in the cooling cloud with CO_2 to form $CaCO_3$ and water [*Adams*, 1953; *Miller*, 1964]. The reformed carbonates (including other elemental forms of interest, like $^{90}SrCO_3$) [*Toggweiler and Trumbore*, 1985] would be a major component of the fallout material by adhering to various kinds of particulate matter in the condensing cloud [*Adams*, 1955], thereby providing a direct infusion and dissolution of at least some of the $Ca^{14}CO_3$ at the sea surface. These fallout patterns were often spread over vast regions, out to more than 40–80 miles (64–129 km) from the shot point [*Adams*, 1957], and include even greater distances for the shots with greatest yield (i.e., Bravo Shot of Operation Castle in 1954 was the largest test in the region at 15 Mt and produced a vast fallout zone to the northeast) [*Martin and Rowland*, 1982; *Kunkle and Ristvet*, 2013]. It is applicable to note that reactive spherical and "fluffy" structured particles were observed as part of the fallout and were composed partly of carbonates that included reformed calcite [*Nishiwaki*, 1954, 1955; *Adams et al*., 1960], which would be partly composed of bomb-produced ^{14}C. Evidence for significant

^{14}C levels in fallout material can be found with a reconstruction of nuclear bomb neutron flux from the $CaCO_3$ of coral reef sands and sediments at Bikini Atoll [*Lachner et al.*, 2014]. In that study, ^{14}C concentrations greatly exceeded a strict neutron activation of the coral carbonate. Hence, the excess ^{14}C was attributed to other sources, which were most likely atmospheric neutron activation of ^{14}N and γ-ray reaction on ^{18}O, with subsequent incorporation of the ^{14}C into the $CaCO_3$ fallout [*Lachner et al.*, 2014]. In addition and perhaps of significant importance, shots made at or below the sea surface created an enormous volume of water vapor that would likely sequester atmospheric $^{14}CO_2$ directly in the cooling and condensing cloud, which would provide a direct pathway to the sea surface.

Close-in fallout from nuclear tests in these islands was extensive. Radioactive plumes in the sea surface created by multi-megaton shots Yankee and Nectar of Operation Castle were tracked by air and sea [*LeVine and Graveson*, 1954]. The regional study provided a direct connection of contaminated water propagation from shot sites with observations of a strongly cohesive plume structure and a limit to the depth of radioactivity (above the thermocline). Tracking of the plume led to a current speed estimate of $\sim$0.5 mi/h ($\sim$0.2 m·s^{-1}) at 3–4 days after Yankee shot, similar to the current speeds calculated for the transit to Guam. At the time of the surveys, the traversed radioactive plumes were 20–30 miles wide (32–48 km). In addition, some observations made by Japanese researchers south of Bikini Atoll using depth-stratified sampling indicated there were density-gradients transporting contaminated water below the surface which appeared to remain within the mixed layer for extended periods [*Nishiwaki*, 1954; *Miyake and Saruhashi*, 1958].

Modeling the advection of bomb-produced ^{14}C from Bikini and Enewetak effectively validated the hypothesis that the three ^{14}C signals observed in coral at Guam were the result of ocean transport in surface currents (Figure 8 and Movie S1). The close temporal alignment of the modeled Castle signal, coupled with a comparable magnitude and period, provided confidence that fallout material generated during thermonuclear tests led to the ^{14}C signals observed in Guam. Current structure in the mixed layer of the sea surface and density gradients of waters laden with fallout material led to differences in the arrival timing and signal strength. Modeling also provided validation of ^{14}C observations made in corals elsewhere. The findings for Palau indicated there was a significant and rapid advection of ^{14}C to the west from the PPG via subsurface currents of the NEC (Figure 6). The early arrival observed in the Palau coral ^{14}C record was not supported by the current modeling and should have arrived $\sim$1–2 months later. However, a bimodal structure was reflected in the modeling with a hiatus in the arrival of fallout waters centered on mid-1954. Modeling indicated that the initial signal (prior to the hiatus) was entirely Bravo and Romeo Shots. Shifting of the Palau coral ^{14}C record by -0.1 year to match the hiatus led to a more unrealistic arrival (before Guam); hence, it is possible that the timeframe represented in the Palau coral samples was slightly less than originally estimated (Figure 9). The modeled return of the ^{14}C signal (posthiatus) was from Union and Yankee Shots, coupled with the return of Bravo and Romeo via the SECC (Movie S1), which may explain the lengthy spike period.

The initial depths of ^{14}C from close-in fallout at the PPG used in the modeling provided some preliminary information on how density gradients may have played a role in transport. Sources of the ^{14}C signal originating in the uppermost depth strata seemed to play a less important role across the western Pacific and may be the result of either advection away from the existing coral records, or at-depth density gradients maintaining a long period of cohesiveness, or both. The ^{14}C record at Okinawa provided some evidence that the pooling effects of the NPG contributed to the moderate, long-period signal observed in this location. The deep origins of the ^{14}C signal at Palau, located on the south side of the NEC, seems to confirm the partitioning of upper fallout ^{14}C layers toward the north. In addition, the passage of bomb-produced ^{14}C to the Langkai and Lombok locations revealed some agreement in timing and a greater contribution from deeper fallout origins (Figure 10). Some of the disagreement in timing for these records may be attributed to the relatively coarse spatial resolution of the SODA currents (more applicable to high-seas transport). However, SODA has been used in other studies of the ITF [*Potemra*, 2005], and is thought to perform well in estimating total transport through this complex region. Further, the simulation modeling was able to show particles utilizing the primary pathways of Lombok Strait, Ombai Strait, and Timor Passage to reach the Indian Ocean, as would be expected based upon oceanographic knowledge of that region [*Bray et al.*, 1997]. Despite the early arrivals, the modeling provided a general validation of the hypotheses that the largest signals at Langkai and Lombok were from close-in fallout of Operation Castle [*Fallon and Guilderson*, 2008;

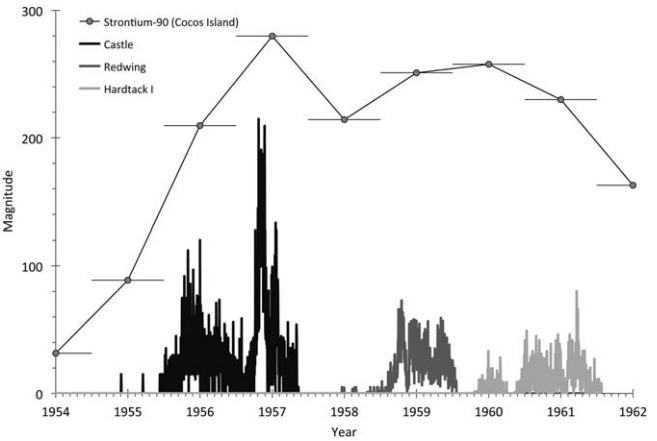

Figure 11. Alignment of the modeled arrival time and magnitude of the plume from each thermonuclear test operation relative to a strontium-90 (^{90}Sr) signal that was recorded in a coral core from Cocos Island in the Indian Ocean [*Toggweiler and Trumbore*, 1985]. Magnitude is modeling counts and an arbitrarily transformed value for the coral ^{90}Sr record to emphasize temporal alignment.

Guilderson et al., 2009]. Furthermore, the modeling confirmed the arrival of contaminated waters at Cocos Island in the Indian Ocean via the ITF, as was postulated from observations of ^{90}Sr levels in a coral record beginning in 1954–1955 (Figure 11) [*Toggweiler and Tumbore*, 1985]. This observation also aligns with what appears to be a small, early ^{14}C spike recorded in a Cocos Island coral for the years 1955–1958 [*Hua et al.*, 2005].

The original goal of this analysis was to provide a bomb ^{14}C benchmark for Guam to be used in answering questions of age for regional fishes. The unusual ^{14}C spikes measured in this study will complicate use of this tool in age validation studies. As is typical with the bomb ^{14}C dating approach, Δ^{14}C measurements from extracted samples will need to consider the possibilities for temporal alignment with the Δ^{14}C reference record. In most cases, the Δ^{14}C rise period (late 1950s to the mid-1960s) is the most diagnostic period because the range of elevated Δ^{14}C values is unique through recent time. The exception in some existing studies is when the Δ^{14}C decline (typically more recent than ~1980) begins to provide a more recent temporal alignment of the measured values, creating a potentially ambiguous result. However, in most cases where this was a potential problem, other information about the time of capture or age and growth can lead to an objective birth year selection [e.g., *Andrews et al.*, 2012, 2013]. When considering the Guam coral record, the complication is most significant with the ^{14}C spike in 1954–1955 because of its amplitude, but is further complicated by the smaller peaks in 1956–1957 and 1958–1959 (Figure 4). In general, the Δ^{14}C rise period would normally provide validated birth years for ~1956–1968 (Δ^{14}C from ~–25 to 115‰), but there is a possibility of birth years in 1954–1955 for any measured Δ^{14}C value in this range because of the Operation Castle spike. The smaller peaks attributed to Operations Redwing and Hardtack I must also be considered for Δ^{14}C values below 3‰ and 30‰, respectively. To overcome these complications, successive sampling into more recent material can provide answers for most of the Δ^{14}C rise, and most effectively for values between 30 and 115‰, where the 1954–1955 spike is widely separated in time from the air-diffusion Δ^{14}C rise period. In addition, further utility of bomb radiocarbon dating of younger fishes collected recently may be aged using the post-peak decline period, as was the case for a coral record established in the Gulf of Mexico [*Andrews et al.*, 2013] and in other places that have a steep post-peak Δ^{14}C decline gradient [*Andrews et al.*, 2016]. The Guam record is more limited in this regard due to the moderately broad peak and may provide diagnostic birth years more recent than 1990, whereas the Gulf of Mexico and Kure Atoll records begin a significant decline in the early 1980s. In addition, the Guam record ends in the year 2000 and would need to be supplemented with more recent known-age carbonates from the region to become more useful in age validation studies (i.e., archived juvenile otoliths) [*Andrews et al.*, 2016].

Acknowledgments

Thank you to S. Kawakami, T. Matsumori, S. Tamashiro, and M. Tsuchiya for assistance with milling extractions at the University of the Ryukyus, Okinawa. Thank you to D. Glynn and E. R. M. Druffel for sharing details of the Palau coral ^{14}C data. Special thanks to K. Elder and A. McNichol at NOSAMS for timely processing of the extensive number of ^{14}C samples used in this study. Thank you to B. Barnett of Panama City Laboratory (NOAA Fisheries, SEFSC) for assistance with constructing the regional base-map of the central and western tropical Pacific in ArcView. Thank you to J. Potemra and N. Fučkar for assistance with the SODA data profiling. Thank you to E. R. M. Druffel and J. R. Toggweiler for reviewing the manuscript and providing constructive comments. Supporting data are included in the associated Supporting Information file and measured carbon isotope data are available at the National Centers for Environmental Information, NESDIS, NOAA, U.S. Department of Commerce; https://www.ncdc.noaa.gov/paleo/study/20346). This study was partly supported by the NMFS Saltonstall Kennedy program (NA14NMF4270056 to F. Camacho and A. Andrews) and the JSPS KAKENHI (26707028 and 26550012 to R. Asami, and 25247083 to Y. Iryu). Dedicated to the late Uncle Frank G. Andrews for his lifetime of inspiration.

References

Adams, C. E. (1953), The nature of individual radioactive particles, II. Fall-out particles from M-shot, Operation Ivy, *Res. Dev. Tech. Rep. USNRDL-408*, 18 pp., U.S. Nav. Radiol. Defense Lab., San Francisco, Calif.

Adams, C. E. (1955), The nature of individual radioactive particles, IV. Fall-out particles from the first shot, Operation Castle, *Res. Dev. Tech. Rep. USNRDL-TR-26*, 23 pp., U.S. Nav. Radiol. Defense Lab., San Francisco, Calif.

Adams, C. E. (1957), The nature of individual radioactive particles, V. Fallout particles from Zuni and Tewa, Operation Redwing, *Res. Dev. Tech. Rep. USNRDL-TR-133*, 16 pp., U.S. Nav. Radiol. Defense Lab., San Francisco, Calif.

Adams, C. E., N. H. Farlow, and W. R. Schell (1960), The compositions, structures and origins of radioactive fall-out particles, *Geochim. Cosmochim. Acta*, *18*, 42–56.

Anderson, E. C., W. F. Libby, S. Weinhouse, A. F. Reid, A. D. Kirshenbaum, and A. V. Grosse (1947), Radiocarbon from cosmic radiation, *Science*, *105*, 576–577.

Andrews, A. H., J. M. Kalish, S. J. Newman, and J. M. Johnston (2011), Bomb radiocarbon dating of three important reef–fish species using Indo–Pacific Δ^{14}C chronologies, *Mar. Freshwater Res.*, *62*, 1259–1269.
Andrews, A. H., E. E. DeMartini, J. Brodziak, R. S. Nichols, and R. L. Humphreys (2012), A long-lived life history for a tropical, deep-water snapper (*Pristipomoides filamentosus*): Bomb radiocarbon and lead-radium dating as extensions of daily increment analyses in otoliths, *Can. J. Fish. Aquat. Sci.*, *69*, 1850–1869.
Andrews, A. H., B. K. Barnett, R. J. Allman, R. P. Moyer, and H. D. Trowbridge (2013), Great longevity of speckled hind (*Epinephelus drummondhayi*), a deep-water grouper, with novel use of post-bomb radiocarbon dating in the Gulf of Mexico, *Can. J. Fish. Aquat. Sci.*, *70*, 1131–1140.
Andrews, A. H., J. H. Choat, R. J. Hamilton, and E. E. DeMartini (2015), Refined bomb radiocarbon dating of two iconic fishes of the Great Barrier Reef, *Mar. Freshwater Res.*, *66*, 305–316.
Andrews, A. H., D. Siciliano, D. Potts, E. E. DeMartini, and S. Covarrubias (2016), Bomb radiocarbon and the Hawaiian Archipelago: Coral, otoliths and seawater, *Radiocarbon*, *58*(3), 531–548.
Asami, R., T. Yamada, Y. Iryu, C. P. Meyer, T. M. Quinn, and G. Paulay (2004), Carbon and oxygen isotopic composition of a Guam coral and their relationships to environmental variables in the western Pacific, *Palaeogeogr. Palaeoclimatol. Palaeoecol.*, *212*, 1–22.
Asami, R., T. Yamada, Y. Iryu, T. M. Quinn, C. P. Meyer, and G. Paulay (2005), Interannual and decadal variability of the western Pacific sea surface condition for the years 1787–2000: Reconstruction based on stable isotope record from a Guam coral, *J. Geophys. Res.*, *110*, C05018, doi:10.1016/j.palaeo.2004.05.014.
Bray, N. A., S. E. Wijffels, J. C. Chong, M. Fieux, S. Hautala, G. Meyers, and W. M. L. Morawitz (1997), Characteristics of the Indo-Pacific throughflow in the eastern Indian Ocean, *Geophys. Res. Lett.*, *24*, 2569–2572.
Broecker, W. S., and A. Walton (1959), Radiocarbon from nuclear tests, *Science*, *130*, 309–314.
Broecker, W. S., and T.-H. Peng (1982), *Tracers in the Sea*, 690 pp., Lamont-Doherty Geol. Obs., Columbia Univ., Palisades, N. Y.
Carton, J. A., G. Chepurin, X. Cao, and B. Giese (2000), A simple ocean data assimilation analysis of the global upper ocean 1950–95, Part I: Methodology, *J. Phys. Oceanogr.*, *30*, 294–309.
Cook, M., G. R. Fitzhugh, and J. S. Franks (2009), Validation of yellow edge grouper, *Epinephelus flavolimbatus*, age using nuclear bomb-produced radiocarbon, *Environ. Biol. Fishes*, *86*, 461–472.
Darrenougue, N., P. De Deckker, C. Payri, S. Eggins, and S. Fallon (2013) Growth and chronology of the rhodolith-forming, coralline red alga *Sporolithon durum*, *Mar. Ecol. Prog. Ser.*, *474*, 105–119.
Department of Energy (1994), United States nuclear tests – July 1945 through September 1992, *NV-209 (Rev. 14)*, 38 pp., U.S. Dep. of Energy, Nev. Oper. Off., National Technical Information Service, U.S. Department of Commerce, Springfield, Va.
Druffel, E. R. M. (1987), Bomb radiocarbon in the Pacific: Annual and seasonal timescale variations, *J. Mar. Res.*, *45*, 667–698.
Druffel, E. R. M. (1997), Geochemistry of corals: Proxies of past ocean chemistry, ocean circulation, and climate, *Proc. Natl. Acad. Sci. U. S. A.*, *94*, 8354–8361.
Druffel, E. R. M. (2002), Radiocarbon in corals: RECORDS of the carbon cycle, surface circulation and climate, *Oceanography*, *15*, 122–127.
Druffel-Rodriguez, K. C., D. Vetter, S. Griffin, E. R. M. Druffel, R. B. Dunbar, D. A. Mucciarone, L. A. Ziolkowski, and J.-A. Sanchez-Cabeza (2012), Radiocarbon and stable isotopes in Palmyra corals during the past century, *Geochim. Cosmochim. Acta*, *82*, 154–162.
Fallon, S. J., and T. P. Guilderson (2005), Extracting growth rates from the nonlaminated coralline sponge *Astosclera willeyana* using bomb radiocarbon, *Limnol. Oceanogr. Methods*, *3*, 455–461.
Fallon, S. J., and T. P. Guilderson (2008), Surface water processes in the Indonesian throughflow as documented by high resolution coral Δ^{14}C, *J. Geophys. Res.*, *113*, C09001, doi:10.1029/2008JC004722.
Gladeck, F. R., et al. (1952), Operation Ivy 1952, *DNA–6036F*, 360 pp., Defense Nucl. Agency, Washington, D. C.
Glasstone, S. (1964), *The Effects of Nuclear Weapons*, *Dep. Army Pamphlet 39–3*, Revised ed., 730 pp., Dep. of Defense and the At. Energy Commiss., Washington, D. C.
Glynn, D., E. Druffel, S. Griffin, R. Dunbar, M. Osborne, J. A. Sanchez-Cabeza (2013), Early bomb radiocarbon detected in Palau Archipelago corals, *Radiocarbon*, *55*, 1659–1664.
Grottoli, A. G., and C. M. Eakin (2007), A review of modern coral δ^{18}O and Δ^{14}C proxy records, *Earth Sci. Rev.*, *81*, 67–91.
Guilderson, T. P., D. P. Schrag, M. Kashgarian, and J. Southon (1998), Radiocarbon variability in the western equatorial Pacific inferred from a high-resolution coral record from Nauru Island, *J. Geophys. Res.*, *103*, 24,641–24,650.
Guilderson, T. P., S. Fallon, M. D. Moore, D. P. Schrag, and C. D. Charles (2009), Seasonally resolved surface water Δ^{14}C variability in the Lombok Strait: A coralline perspective, *J. Geophys. Res.*, *114*, C07029, doi:10.1029/2008JC004876.
Hansen C. (1988), *US Nuclear Weapons - The Secret History*, 232 pp., Aerofax, Inc., Arlington, Tex.
Hawthorne, H. A. (1979), Compilation of local fallout data from test detonations 1945-1962—Extracted from DASA 1251, *DNA-1251-2-EX*, 334 pp., Defense Nucl. Agency., Washington, D. C.
Hua, Q., C. D. Woodroffe, S. G. Smithers, M. Barbetti, and D. Fink (2005), Radiocarbon in corals from the Cocos (Keeling) Islands and implications for Indian Ocean circulation, *Geophys. Res. Lett.*, *32*, L21602, doi:10.1029/2005GL023882.
Hua, Q., M. Barbetti, and A. Z. Rakowski (2013), Atmospheric radiocarbon for the period 1950-2010, *Radiocarbon*, *55*, 2059–2072.
Kalish, J. M. (1993), Pre- and post-bomb radiocarbon in fish otoliths, *Earth Planet. Sci. Lett.*, *114*, 549–554.
Konishi, K., T. Tanaka, and M. Sakanoue (1982), Secular variation of radiocarbon concentration in seawater: Sclerochronological approach, in *Proceedings of the Fourth International Coral Reef Symposium*, vol. 1, pp. 181–185.
Kunkle, T., and B. Ristvet (2013), *Castle Bravo: Fifty Years of Legend and Lore*, 183 pp., Defense Threat Reduction Agency, Kirtland, Tex.
Lachner, J., M. Christl, V. Alfimov, I. Hajdas, P. W. Kubik, T. Schultz-König, L. Wacker, and H.-A. Synal (2014), ^{41}Ca, ^{14}C and ^{10}Be concentrations in coral sand from Bikini atoll, *J. Environ. Radioact.*, *129*, 68–72.
Latter, A. L., and M. S. Plesset (1960), Carbon-14 production from nuclear explosions, *Proc. Nat. Acad. Sci. U. S. A.*, *46*, 241–247.
LeVine, H. D., and R. T. Graveson (1954), Radioactive debris from Operation Castle aerial survey of open sea following Yankee-Nectar, *NYO-4618*, 62 pp., U.S. At. Energy Commiss., N. Y. Oper. Off., Washington, D. C.
Libby, W. F. (1946), Atmospheric helium three and radiocarbon from cosmic radiation, *Phys. Rev.*, *69*, 671–672.
Libby, W. F. (1955), *Radiocarbon Dating*, 2nd ed., 175 pp., Univ. of Chicago Press, Chicago, Ill.
Libby, W. F. (1957), Radioactive fallout, *Proc. Natl. Acad. Sci. U. S. A.*, *43*, 758–775.
Libby, W. F. (1958), Radioactive fallout, *Proc. Natl. Acad. Sci. U. S. A.*, *44*, 800–820.
Lindahl, P., R. Asami, Y. Iryu, P. Worsfold, M. Keith-Roach, and M.-S. Choi (2011), Sources of plutonium to the tropical northwest Pacific Ocean (1943–1999) identified using a natural coral archive, *Geochim. Cosmochim. Acta*, *75*, 1346–1356, doi:10.1016/j.gca.2010.12.012.
Martin, E. J., and R. H. Rowland (1982), United States atmospheric nuclear weapons tests, nuclear test personnel review, in *Castle Series*, *Rep. DNA–6035F*, 526 pp., Defense Nuclear Agency, Washington, D. C.

Miller, C. F. (1964), *Biological and Radiological Effects of Fallout From Nuclear Explosions*, 82 pp., Stanford Res. Inst., Menlo Park, Calif.
Mitsuguchi, T., X. D. Phong, H. Kitagawa, M. Yoneda, and Y. Shibata (2007), Tropical South China Sea surface ^{14}C record in an annually banded coral, *Radiocarbon*, *49*, 905–914.
Miyake, Y., and K. Saruhasi (1958), Distribution of man-made radioactivity in the North Pacific through summer 1955, *J. Mar. Res.*, *17*, 383–389.
Moore, M. D., D. P. Schrag, and M. Kashgarian (1997), Coral radiocarbon constraints on the source of the Indonesian throughflow, *J. Geophys. Res.*, *102*, 12,359–12,365.
Nishiwaki, Y. (1954), Bikini ash, *At. Sci. J. UK*, *4*, 97–109.
Nishiwaki, Y. (1955), Effects of H-bomb tests in 1954, *At. Sci. J. UK*, *4*, 279–288.
Nydal, R. (1968), Further investigation on the transfer of radiocarbon in nature, *J. Geophys. Res.*, *73*, 3617–3635.
Nydal, R., and J. S. Gislefoss (1996), Further application of bomb ^{14}C as a tracer in the atmosphere and ocean, *Radiocarbon*, *38*, 389–406.
Potemra, J. T. (2005), Indonesian Throughflow transport variability estimated from satellite altimetry, *Oceanography*, *18*, 98–107.
Reimer, P. J., T. A. Brown, and R. W. Reimer (2004), Discussion: Reporting and calibration of post-bomb ^{14}C data, *Radiocarbon*, *46*, 1299–1304.
Rivera, M. A. J., K. R. Andrews, D. R. Kobayashi, J. L. K. Wren, C. Kelley, G. K. Roderick, and R. J. Toonen (2011), Genetic analyses and simulations of larval dispersal reveal distinct populations and directional connectivity across the range of the Hawaiian grouper (*Epinephelus quernus*), *J. Mar. Biol.*, *2011*, 765353.
Sevitt, S. (1955), The bombs, *Lancet*, 199–201.
Shinjo, R., R. Asami, K.-F. Huang, C.-F. You, and Y. Iryu (2013), Ocean acidification trend in the tropical North Pacific since the mid-20th century reconstructed from a coral archive, *Mar. Geol.*, *342*, 58–64, doi:10.1016/j.margeo.2013.06.002.
Stuiver, M., and H. A. Polach (1977), Discussion: Reporting of ^{14}C data, *Radiocarbon*, *19*, 355–363.
Southon, J., M. Kashgarian, M. Fontugne, B. Metivier, and W. W.-S. Yim (2002), Marine reservoir corrections for the Indian Ocean and Southeast Asia, *Radiocarbon*, *44*, 167–180.
Toggweiler, J. R., and S. Trumbore (1985), Bomb-test ^{90}Sr in Pacific and Indian Ocean surface water as recorded by banded corals, *Earth Planet. Sci. Lett.*, *74*, 306–314.
Van Houtan, K. S., A. H. Andrews, T. T. Jones, S. K. K. Murakawa, and M. E. Hagemann (2016), Time in tortoiseshell: A bomb radiocarbon-validated chronology in sea turtle scutes, *Proceedings of the Royal Society B*, *283*(1822): 2015–2220.
Vitale, S., A. H. Andrews, P. Rizzo, S. Gancitano, and F. Fiorentino (2016), Twenty-five-year longevity of European hake (*Merluccius merluccius*) from novel use of bomb radiocarbon dating in the Mediterranean Sea, *Mar. Freshwater Res.*, *67*, 1077–1080, doi:10.1071/MF15376.
Wessel, P., and W. H. F. Smith (1991), Free software helps map and display data, *Eos Trans. AGU*, *72*, 441–446.
Wren, J. L. K., and D. R. Kobayashi (2016), Exploration of the ''larval pool'': Development and ground-truthing of a larval transport model off leeward Hawai'i, *PeerJ*, *4*, e1636.
Yang, X., R. North, C. Romney, and P. G. Richards (2000), Worldwide nuclear explosions, *Tech. Rep. CMR-00/16*, 92 pp., Cent. for Monit. Res., Arlington, Va. [Available at https://www.ldeo.columbia.edu/~richards/my_papers/WW_nuclear_tests_IASPEI_HB.pdf.]